White Rose
university consortium
Universities of Leeds, Sheffield & York

eprints@whiterose.ac.uk
https://eprints.whiterose.ac.uk/

A NOVEL HYBRID SEMI-ACTIVE TUNED MASS DAMPER FOR LIGHTWEIGHT STEEL STRUCTURAL APPLICATIONS

Demetris Demetriou*, Nikolaos Nikitas* and Konstantinos Daniel Tsavdaridis*

* University of Leeds, School of Civil Engineering, United Kingdom
cn09dd@leeds.ac.uk, N.Nikitas@leeds.ac.uk, K.Tsavdaridis@leeds.ac.uk

Keywords: Vibration control; Semi-active; Hybrid vibration mitigation systems; High-rise structures

Abstract. This paper proposes the application of a novel hybrid semi-active vibration absorber for the control of multistorey vibration prone structures under wind excitation. It is shown that the novel device outperforms the traditional tuned mass damper (TMD) by achieving performance gains similar to an active mass damper (AMD) while maintaining robustness at the extra benefit of considerably less energy and actuation demands, satisfying both strict serviceability and sustainability requirements often govern most lightweight steel structural applications.

1 INTRODUCTION

Almost a century after the invention of the dynamic vibration absorber (DVA), tuned mass dampers (TMD) are found to be amongst the most popular methods for civil engineering structural control. While TMDs have been shown to be successful at alleviating structural response under generic dynamic loading, such devices being tuned to a single vibration mode of the structure are limited to a narrow band of operating frequencies that in turn could compromise the system's attenuation capacity when excited beyond this targeted mode. Additionally, such devices being sensitive to de-tuning either as a result of material degradation, structural damage or simply due to bad modelling practices, compromise further their vibration attenuation capacity. In this regard, over the last few decades, attempts have been made to improve the performance of the traditional passive TMD by substituting its passive elements with active and semi-active components. Clearly, active mass dampers (AMD) have been shown to outperform purely passive and semi-active dampers (STMD) when it comes to vibration attenuation, yet this performance enhancement comes at the expense of considerable power -force demands and reliability. As a result, hybrid mass dampers (HMDs) (these being purely passive TMDs working in conjunction with active control elements) are found in many practical applications. Studies such as [1-3] are a few amongst the many illustrating the performance gains of the use of HMDs on structural systems under both earthquake and wind excitations. Yet, similarly to the AMD the performance objective is achieved at the expense of considerable power demands.

In this study, the limitations of the TMD, AMD and HMD are surpassed through the use of a novel semi-active hybrid mass damper (SHMD) proposed by the authors. This device extends the conventional HMD logic by making use of an STMD working in conjunction with actively controlled elements. The performance gains from the use of this novel SHMD device are illustrated through a comparative study on a 76-storey wind excited benchmark sway structure equipped with passive, active and semi-active tuned mass dampers.

2 MODELING PRINCIPLES

2.1 Modeling of passive/active and semi-active dampers

Modelling the novel SHMD device requires a thorough understanding of the modelling principles of its passive, active and semi-active counterparts. Starting from the straightforward passive system, the operational principle of a simple TMD can be explained by considering a simple n-DOF sway structure as the one depicted in Fig. 1. The dynamic behaviour of such a system when subjected to an arbitrary disturbance is fully captured by its matrix equation of motion:

$$M\ddot{x}(t) + C\dot{x}(t) + Kx(t) = Bu(t) + Dd(t) \tag{1}$$

where each overdot declares single differentiation with respect to t, M, C and K are the $n \times n$ mass, damping, and stiffness matrices respectively; $x(t)$ and $d(t)$ are in order the displacement, and external force $n \times 1$ column vectors; $u(t)$ is the single scalar control force and B ($n \times 1$) and D ($n \times n$) are the influence matrices assigning the control and external force contributions respectively to the individual DOFs. For each DOF in $x(t)$ being the lateral displacement of the ith ($i = 1, ..., n$) mass, M trivially becomes diagonal, while for the classical viscous damping considered (and connections as in Fig. 1) the damping matrix C attains a form identical to the symmetric stiffness matrix K. Without any loss of generality the mass damper device is attached to the $(n-1)^{th}$ DOF and its motion constitutes the nth DOF.
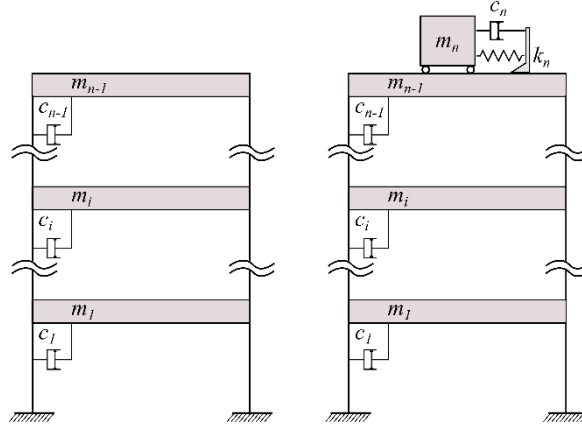

Figure 1: Simple $(n-1)$-storey example building where a TMD is employed.

The matrix Eq. (1) could describe a system equipped with any type of viscous dynamic absorbing device. The difference between the passive, active and semi-active schemes would exclusively be captured by the nature of the control force $u(t)$. It would be probably more appropriate for the passive case to term $u(t)$ as the interaction force, yet for economy in presentation and homogeneity, the term control is used throughout. To facilitate the derivation of a semi-active control force, it would be beneficial to first consider the case of a purely passive TMD. When the TMD is attached to the system of interest $u(t)$ takes the form of a purely passive action, $u_p(t)$ resulting solely from the motion of the absorber's mass. This passive force which couples the damper to the rest of the system can be mathematically expressed as:

$$u_p(t) = c_n \dot{x}_r(t) + k_n x_r(t) \tag{2}$$

In Eq. (2) , c_n is the constant scalar damping coefficient and k_n is the constant scalar spring stiffness of the TMD (as depicted in Fig. 1), while $\dot{x}_r(t)$ and $x_r(t)$ are respectively the relative velocity and displacement between the nth and $(n-1)^{th}$ DOFs. It should be also noted that the n-element B matrix becomes $[0... \; 1 \; -1]^T$. When an active control system is considered, the control force takes the form of a desired action, $u_a(t)$ determined via a control algorithm such as the Linear-Quadratic-Regulator (LQR), PID or any similar control algorithm. For an AMD, the desired force is the summation of the passive forces generated by the mass damper's motion and an additional external force provided by means of mechanical actuation. Because the dynamic characteristics of the mass damper remain unaltered and the desired interaction force, $u_a(t)$ has been already calculated by the control algorithm, the required actuation force, $f_a(t)$ can be readily determined from:

$$u_a(t) = c_n \dot{x}_r(t) + k_n x_r(t) - f_a(t) \tag{3}$$

For purely active systems, the values of c_n and k_n can take zero values, resulting to the control action to be equal to the actuation force:

$$u_a(t) = -f_a(t) \tag{4}$$

However, the requirement of a fail-safe mechanism dictates that in most practical applications the values of c_n and k_n would be of similar magnitude to the passive TMD equivalents. The resulting system that combines the passive TMD and the purely active AMD (see Eq. (3)) is known as a hybrid system.

For the case of semi-active control, obtaining the control action involves the calculation of an equivalent active force which at the same time can be physically realised by the semi-active device. In this regard, because of the fact that no energy can be added directly to the system, the semi-active device will produce control forces only when required i.e. when the damper is requested to "consume" energy. Having already obtained an equivalent active force from Eq. (4), the final step is to apply semi-active force saturation limits such that the semi-active control force, $u_{sa}(t)$ is calculated by [4]:

$$u_{sa}(t) = f_a(t) \left(\frac{1 - \text{sgn}[f_a(t)\dot{x}_r(t)]}{2} \right) \tag{5}$$

$$\text{sgn}[f_a(t)\dot{x}_r(t)] = \text{sgn}(q_a(t)) = \begin{cases} 1 & \text{for} \quad q_a \geq 0 \\ -1 & \text{for} \quad q_a < 0 \end{cases} \tag{6}$$

The product of $f_a(t)\dot{x}_r(t)$ is the power, q_a, of the whole active system device. Similarly, the power of just the semi-active component is defined as the product of the force that can be physically translated by the device, $u_{sa}(t)$ and its relative velocity, $\dot{x}_r(t)$:

$$q_{sa}(t) = u_{sa}(t)\dot{x}_r(t) < 0 \tag{7}$$

A schematic representation of the power time histories of both an actively and a semi-actively controlled devices is shown in Fig. 2. It can be observed that the active device has the advantage of both negative and positive powers, while the semi-active device only consumes power. This reinforces the fact that an active control scheme can potentially also add energy to the system whereas a semi-active scheme can only dissipate energy.
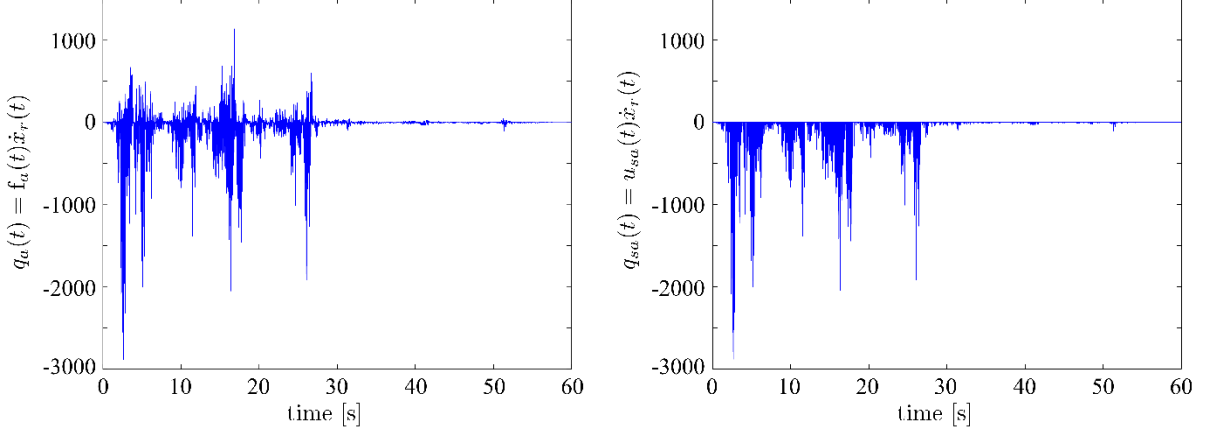

Figure 2: Indicative example of the "power" scheme/demand practiced in semi-active control (see Eqs. (5-7)). The device only performs to dissipate energy (q_a , q_{sa} in Watt).

So far, the principle of obtaining a "desired" control force to be provided by a semi-active device has been discussed. When a variable damping (VD) STMD is considered, the chosen way of achieving optimum performance is by appropriately timely adjusting the damping coefficient of the device within bands, in order for the required control force to be reached. By referring back to the system presented in Fig. 1, one can express the semi-active damping force contribution as $c_{sa}(t) \, \dot{x}_r(t)$. An inspection of Eq. (7) easily leads to $c_{sa}(t) < 0$. Updating Eq. (3), the resulting overall control force provided at each time instant by a VD-STMD can be expressed mathematically as:

$$u_a(t) = (\left|c_{sa}(t)\right| + c_n)\dot{x}_r(t) + k_n x_r(t) \tag{8}$$

In Eq. (8) the time varying semi-active damping coefficient, $c_{sa}(t)$ is the only unknown. Therefore, calculating the real-time variation of the damping coefficient is straightforward.

2.2 Modeling the semi-active hybrid mass damper

Through the use of a SHMD the energy dissipation capacity of a semi-active device is exploited and energy is added only when required through force actuators. The main difference between an AMD and a SHMD lies in the fact that the actuators of the AMD both add and dissipate energy whereas the forcing provision of the SHMD can only add energy. It is worth noting that dissipating energy using active actuators requires power of the order of kWatt, whereas dissipating energy using semi-active devices requires power of just a few Watt [5]. The steps required for the calculation of the envisaged control action, $u_{shmd}(t)$ are:

1. Calculation of an active force according to Eq. (4) via an appropriate control algorithm
2. Calculation of an equivalent semi-active force using Eq. (5) based on the active force, $f_a(t)$ calculated using active algorithms such as the LQR or similar algorithm. Alternatively, direct output feedback control algorithms such the ones found in the groundhook scheme can be used to alleviate the online computational burden of Eq. (5) (see section 3).

3. Calculate an additional active force using strictly active control algorithms and limit the capacity of the actuator such that it can only add power:

$$q_a(t) = f_a(t)\dot{x}_r(t) > 0 \tag{9}$$

It is noteworthy, that enabling performance of the actuator can be achieved by using Eq. (5) and simply inverting the sign conditions of Eq. (6) such that:

$$\text{sgn}(q_a(t)) = \begin{cases} 1 & \text{for} \quad q_a \leq 0 \\ -1 & \text{for} \quad q_a > 0 \end{cases} \tag{10}$$

Alternatively, performance conditions/limitations can be placed using a direct output control algorithm (groundhook) (see section 3).

4. Incorporate both active and semi-active forces to the system using:

$$u_{shmd}(t) = u_{sa}(t) + f_a(t) \tag{11}$$

3 CONTROL METHODS

As discussed in the previous sections, obtaining the semi-active and active actions is achieved via control algorithms. For the purely active control case, the algorithm of choice is the LQR whereas for the case of semi-active control the algorithm of choice is the velocity based groundhook algorithm which belongs to the category of direct output feedback controllers (i.e. the control actions are calculated based on a limited number of measurements). The choice of direct output feedback controller for the case of semi-active control is based on the reduction of computational effort required for the online calculation of Eqs. (5) and (6).

3.1 Semi-active control / Groundhook

In a groundhook control scheme, the directionality condition of the forces needs to be examined in order to determine the required control action. Depending on the motion of the mass of the damper and the structure and without the loss of generality, four cases are identified and damper forces are calculated in accordance to Table 1 [6]:

Table 1: Groundhook Control strategy.

Sign convention	Damper conditions	Desired damping state
$\dot{x}_{n-1} > 0, \quad \dot{x}_r < 0$	Extension	Off
$\dot{x}_{n-1} > 0, \quad \dot{x}_r > 0$	Compression	On
$\dot{x}_{n-1} < 0, \quad \dot{x}_r < 0$	Extension	On
$\dot{x}_{n-1} < 0, \quad \dot{x}_r > 0$	Compression	Off

Summarising the conditions, this velocity based groundhook (VBG) control rationale is mathematically captured by:

$$\dot{x}_{n-1}\dot{x}_r \geq 0 \qquad c_{sa}(t) = \text{Max} \tag{12}$$

$$\dot{x}_{n-1}\dot{x}_r < 0 \qquad c_{sa}(t) = Min \tag{13}$$

Alternatively, it is possible to replace the velocity of the unsprung damper mass by a primary system displacement term, resulting to displacement based (DBG) control, mathematically expressed as:

$$x_{n-1}\dot{x}_r \geq 0 \qquad c_{sa}(t) = Max \tag{14}$$

$$x_{n-1}\dot{x}_r < 0 \qquad c_{sa}(t) = Min \tag{15}$$

The semi-active control force is thus calculated by:

$$u_{sa}(t) = c_{sa}(t)\dot{x}_r \tag{16}$$

3.2 Active control / LQR

The LQR works on the basis of minimising a quadratic performance index through manipulation and optimisation of the control input vector $Bu(t)$, see Eq. (1). The performance index used in structural control applications when working with the state space formulation is defined as [7]:

$$J = \int_0^{tf} [x^T(t)Qx(t) + (Bu(t))^T R(Bu(t))]dt \tag{17}$$

In Eq. (17), Q and R are weighting matrices relating to the trade-off between control effectiveness and control energy consumption respectively, tf is the control period of consideration. By manipulating the magnitudes of Q and R, better disturbance rejection can be achieved at the expense of control effort and vice versa. For example, a better disturbance rejection and minimization of the state error could be achieved by increasing the magnitude of the elements of the Q matrix relative to the R matrix. In contrast, increasing the magnitude of the R relative to the Q matrix would yield smaller control forces thus less control effort as well as reduced disturbance rejection. The values of elements of these matrices are selected such that Q is a positive semi-definite matrix and R is a positive definite matrix. By doing so, Eq. (17) will never yield a negative result. Once the weighting matrices have been obtained, the problem reduces to the classical optimal problem where the control gain G is calculated by:

$$G = -\frac{1}{2}R^{-1}E^T P \tag{18}$$

where, P is the Riccati matrix found by solving the algebraic Riccati equation:

$$PA - \frac{1}{2}PER^{-1}E^T P + A^T P + 2Q = 0 \tag{19}$$

where A is the system matrix and E is the control force locator matrix in the state space formulation of the dynamic problem (i.e states $X = [x(t) \quad \dot{x}(t)]^T$). i.e.

6

$$A = \begin{bmatrix} 0 & I \\ -M^{-1}K & -M^{-1}C \end{bmatrix}, \qquad E = \begin{bmatrix} 0 \\ M^{-1}B \end{bmatrix} \qquad (20)$$

with I being the identity matrix. When full-state feedback is available, the control force is calculated based on:

$$u(t) = -GX \qquad (21)$$

3.2 Semi-active hybrid control

For the SHMD case the semi-active force component is calculated using a VBG controller, whereas, the active force, component, $u_{active}(t)$ is calculated using a LQR and its capacity is restricted to only producing power in accordance to Eq. (9) via another VBG such that:

$$x_{n-1}\dot{x}_r \geq 0 \qquad u_{active}(t) = u_a(t) \qquad (22)$$

$$x_{n-1}\dot{x}_r < 0 \qquad u_{active}(t) = 0 \qquad (23)$$

4 NUMERICAL INVESTIGATION

4.1 Structural configuration

The effectiveness of the proposed device is illustrated through numerical simulations on the 76-storey benchmark wind-sensitive sway structure proposed by Yang et al. [8]. The structure is excited by across wind loading for a duration of 900s, enough for the response to establish its stationary properties. In this study, four alternatives, namely: passive (TMD), semi-active (STMD), active (AMD) and semi-active hybrid (SHMD) controlled structures were used to demonstrate the performance gains of the new device. The configuration of all the mitigation measures are shown in Fig. 3.
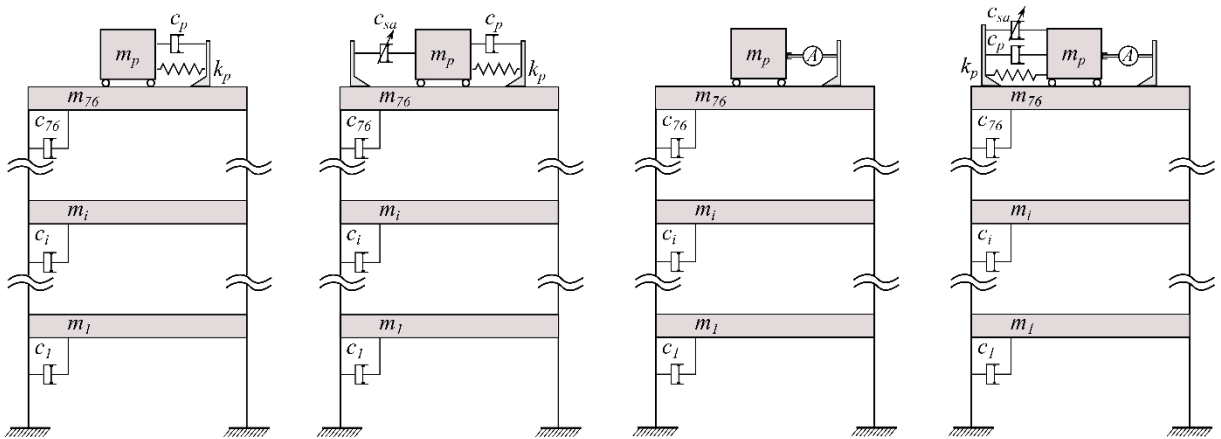

Figure 3: Ensemble of all the different control options (i.e. TMD, STMD, AMD, SHMD) studied herein for the model 76-storey structure of Yang et al. [8].

For the fairness of the comparison the mass of each damper was kept the same (500t), while at the same time it was deemed necessary to restrain the maximum damper stroke of each of the alternatives by increasing the damping coefficient of the device appropriately so

as to limit strokes to a maximum of 95 cm. As a matter of fact, since the damper stroke is the main performance limiting factor, the assessment of the devices that can alter online their damping capacity was performed on the basis of a maximum stroke of 70cm. This is indicated by the performance criterion J_{11} (≈ 2.11) (see section 4.2). The resulting damping coefficients that equalize the maximum strokes are outlined below:

Table 2. Damping coefficients

Control strategy	Max Damping coefficient (kNs/m)	Min Damping coefficient (kNs/m)	Equivalent Damping ratio
TMD	210	210	20%
STMD	145	50	14-5%
AMD	N/A	N/A	N/A
SHMD	105	50	10-5%

4.2 Evaluation criteria

The comparison of the different control strategies is based on the stationary response properties of the different control structures. From the response time histories, the rms and peak accelerations and displacements at different storeys were obtained. From the obtained values, twelve performance criteria were identified. The first criterion, J_1 appraises the ability of the control strategy to reduce rms accelerations:

$$J_1 = \max(\sigma_{\ddot{x}1}, \sigma_{\ddot{x}30}, \sigma_{\ddot{x}50}, \sigma_{\ddot{x}55}, \sigma_{\ddot{x}60}, \sigma_{\ddot{x}65}, \sigma_{\ddot{x}70}, \sigma_{\ddot{x}75}) / \sigma_{\ddot{x}75o} \qquad (24)$$

where $\sigma_{\ddot{x}i}$ is the rms acceleration of the ith storey and $\sigma_{\ddot{x}75o}$ is the rms acceleration of the 75th floor (last occupied floor) without control. The second performance criterion evaluates the average performance of six floors above the 49th floor:

$$J_2 = \frac{1}{6}\sum_i (\sigma_{\ddot{x}i} / \sigma_{\ddot{x}io}); \qquad (25)$$

For $i = 50, 55, 60, 65, 70, 75$; where, $\sigma_{\ddot{x}io}$ is the rms of the ith floor without control. The third and fourth performance indices assess the ability of the control system to reduce top floor displacements:

$$J_3 = \sigma_{x76} / \sigma_{x76o} \qquad (26)$$

$$J_4 = \frac{1}{7}\sum_i (\sigma_{xi} / \sigma_{xio}); \qquad (27)$$

For $i = 50, 55, 60, 65, 70, 75, 76$; where, σ_{xi} is the rms displacement of the ith floor, σ_{xio} is the rms displacement of the ith storey without control and σ_{x76o} is 10.136 cm. The fifth and sixth indices take into account the rms stroke of the damper (i.e. $i = 77$) and the average power respectively:

$$J_5 = \sigma_{x77} / \sigma_{x76o} \qquad (28)$$

$$J_6 = \{\frac{1}{T}\int_0^T [\dot{x}_{77}(t)u(t)]^2 dt\}^{1/2} \tag{29}$$

In which, σ_{x77} is the rms stroke of the damper, $\dot{x}_{77}(t)$ is the damper velocity and T is the total time of integration. Similarly to the first performance indices, the next four criteria (i.e. J_7 to J_{10}) evaluate the performance in terms of peak response quantities:

$$J_7 = max(\ddot{x}_{p1}, \ddot{x}_{p30}, \ddot{x}_{p50}, \ddot{x}_{p55}, \ddot{x}_{p60}, \ddot{x}_{p65}, \ddot{x}_{p70}, \ddot{x}_{p75})/\ddot{x}_{p75o} \tag{30}$$

$$J_8 = \frac{1}{6}\sum_i (\ddot{x}_{pi},/\ddot{x}_{pio},); \tag{31}$$

For $i = 50, 55, 60, 65, 70, 75$;

$$J_9 = x_{p76}/x_{p76o} \tag{32}$$

$$J_{10} = \frac{1}{7}\sum_i (x_{pi}/x_{pio}); \tag{33}$$

For $i = 50, 55, 60, 65, 70, 75, 76$; where, $\ddot{x}_{pi}$ is the peak acceleration of the ith floor with control and $\ddot{x}_{pio}$ is the peak acceleration of the ith floor without control. Similarly, x_{pi} is the peak displacement of the ith floor and x_{pio} is the peak displacement of the ith floor without control. The 11th criterion assesses the ability of the control strategy to minimise the stroke of the damper:

$$J_{11} = x_{p77}/x_{p76o} \tag{34}$$

In which, x_{p77} is the peak stroke of the actuator. The last criterion examines the control effort by calculating the maximum required power by:

$$J_{12} = max|\dot{x}_{77}(t)u(t)| \tag{35}$$

From the above defined criteria, it can be observed that the better the performance, the smaller the performance indices $J_1, J_2, ..., J_{12}$[8].

5 SIMULATION RESULTS AND CONCLUSIONS

Four structural configurations consisting of passive, semi-active, active and semi-active hybrid control devices were considered for investigating the efficacy of the SHMD device for the vibration control of high-rise structures. Fig. 4 summarizes the peak and rms (displacement and acceleration) responses at every floor. The results of the evaluation for the different performance criteria $J_1..J_{12}$ are presented in Table 3.
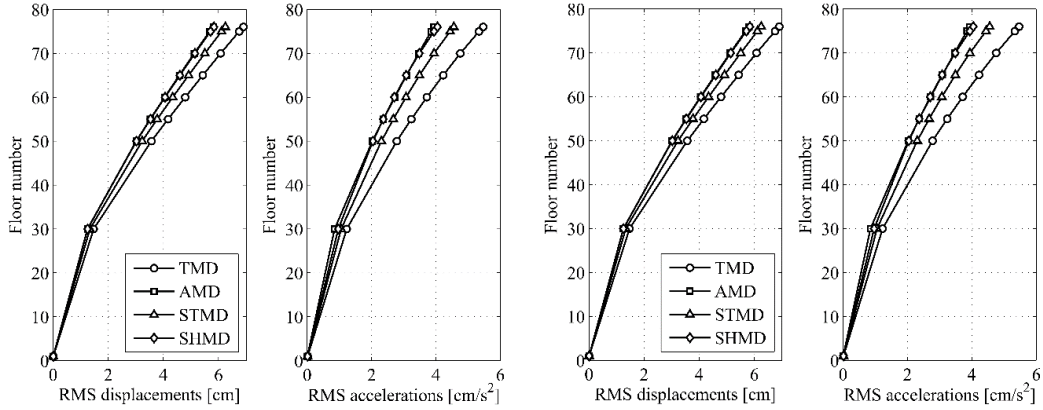
Figure 4: Illustration of the performance of different control measures in terms of displacement and acceleration at different floor levels.

The results indicate that for approximately the same damper strokes, the SHMD equipped structure is able to achieve similar performance to the AMD equipped one, while clearly outperforming the semi-actively controlled alternative. With reference to Table 3, it is also evident that the SHMD device requires much less energy and force demands for achieving the aforementioned performance increase. As a matter of fact, the SHMD device requires approximately 10% of the total energy required by the AMD device. This can be explained by the large amount of energy required to be dissipated by the active actuators (approximately 5400 kJ $\approx$ 2.2 kWh or 75% of the total energy required), which for the case of SHMD control occurs at the expense of a few Wh. Additionally, the active actuators of the SHMD require just 779 kJ $\approx$ 0.2 kWh as opposed to the AMD actuators that require 1915 kJ $\approx$ 0.53 kWh (the remaining 25% of the required energy).

Table 3. Performance criteria overview

Performance index	TMD	STMD	AMD	SHMD
J_1	1.52	2.58	2.85	2.38
J_2	0.58	0.48	0.43	0.42
J_3	0.68	0.62	0.58	0.57
J_4	0.58	0.53	0.50	0.49
J_5	1.26	2.19	2.53	2.09
J_6	N/A	N/A	1.91	9.66
J_7	1.49	2.44	2.31	2.57
J_8	0.64	0.51	0.45	0.41
J_9	0.68	0.57	0.51	0.53
J_{10}	0.59	0.48	0.44	0.45
J_{11}	1.32	2.17	2.15	2.10
J_{12}	N/A	N/A	33.03	54.15
Max $u(t)$ (kN)	N/A	N/A	300	100
Rms $u(t)$ (kN)	N/A	N/A	57.87	64.02
Max $q_a(t)$ (kWatt)	N/A	N/A	57.87	32.09
Rms $q_a(t)$ (kWatt)	N/A	N/A	13.36	2.88
Total added energy (kJ)	N/A	N/A	7315	779

10

6 REFERENCES

[1] Fujinami T, Saito Y, Masayuki M, Koike Y, Tanida K., A hybrid mass damper system controlled by Hinfity control theory for reducing bending-torsion vibration of an actual building. Earthquake Engineering & Structural Dynamics. 2001;30:1639-43.

[2] Watakabe M, Tohdp M, Chiba O, Izumi N, Ebisawa H, Fujita T. Response control performance of a hybrid mass damper applied to a tall building. Earthquake Engineering and Structural Dynamics. 2001;30:1655-76.

[3] Nakamura Y, Tanaka K, Nakayama M, Fujita T. Hybrid mass dampers using two types of electric servomotors:AC servomotors and linear-induction servomotors. Earthquake Engineering and Structural Dynamics. 2001;30:1719-43.

[4] Hrovat D, Barak P, Rabins M. Semi-active versus passive or active tuned mass dampers for structural control. Journal of Engineering Mechanics. 1983;109:691-705.

[5] Nagarajaiah S, Varadarajan N. Short time Fourier transform algorithm for wind response control of buildings with variable stiffness TMD. Engineering Structures. 2005;27:431-41.

[6] Koo JH. Using magneto-rheological dampers in semiactive tuned vibration absorbers to control structural vibrations. Phd thesis, Blacksburg,Virginia: Virginia Polytechnic Institute and State University; 2003.

[7] Soong TT. Active Structural Control: Theory and Practice. New York: John Wiley & Sons,Inc.; 1990.

[8] Yang NY, Agrawal AK, Samali B, Wu JC. Benchmark problem for response control of wind-excited tall buildings. Journal of Engineering Mechanics. 2004;130:437-46.